



Pediatric body composition based on automatic segmentation of computed tomography scans: a pilot study

Atia Samim^{1,2} · Suzanne Spijkers¹ · Pim Moeskops^{3,4} · Annemieke S. Littooi^{1,2} · Pim A. de Jong¹ · Wouter B. Veldhuis^{1,3} · Bob D. de Vos^{3,5} · Hanneke M. van Santen^{2,6} · Rutger A. J. Nievelstein^{1,2}

Received: 24 April 2023 / Revised: 31 July 2023 / Accepted: 1 August 2023 / Published online: 29 August 2023
© The Author(s) 2023

Abstract

Background Body composition during childhood may predispose to negative health outcomes later in life. Automatic segmentation may assist in quantifying pediatric body composition in children.

Objective To evaluate automatic segmentation for body composition on pediatric computed tomography (CT) scans and to provide normative data on muscle and fat areas throughout childhood using automatic segmentation.

Materials and methods In this pilot study, 537 children (ages 1–17 years) who underwent abdominal CT after high-energy trauma at a Dutch tertiary center (2002–2019) were retrospectively identified. Of these, the CT images of 493 children (66% boys) were used to establish normative data. Muscle (psoas, paraspinal and abdominal wall) and fat (subcutaneous and visceral) areas were measured at the third lumbar vertebral (L3) level by automatic segmentation. A representative subset of 52 scans was also manually segmented to evaluate the performance of automatic segmentation.

Results For manually-segmented versus automatically-segmented areas (52 scans), mean Dice coefficients were high for muscle (0.87–0.90) and subcutaneous fat (0.88), but lower for visceral fat (0.60). In the control group, muscle area was comparable for both sexes until the age of 13 years, whereafter, boys developed relatively more muscle. From a young age, boys were more prone to visceral fat storage than girls. Overall, boys had significantly higher visceral-to-subcutaneous fat ratios (median 1.1 vs. 0.6, $P < 0.01$) and girls higher fat-to-muscle ratios (median 1.0 vs. 0.7, $P < 0.01$).

Conclusion Automatic segmentation of L3-level muscle and fat areas allows for accurate quantification of pediatric body composition. Using automatic segmentation, the development in muscle and fat distribution during childhood (in otherwise healthy) Dutch children was demonstrated.

Keywords Body composition · Child · Computed tomography · Sarcopenia · Skeletal muscle · Subcutaneous fat · Visceral fat

Introduction

Body composition, in particular the distribution of skeletal muscle and fat tissue, can be an important predictor of various health outcomes [1]. In adults, for instance, sarcopenia has been associated with increased mortality and morbidity

A. Samim and S. Spijkers contributed equally as co-first authors.

✉ Atia Samim
atiasamim@gmail.com

¹ Department of Radiology and Nuclear Medicine, University Medical Center Utrecht and Wilhelmina Children's Hospital, Heidelberglaan 100, 3584 CX, Utrecht, The Netherlands

² Princess Máxima Center for Pediatric Oncology, Utrecht, The Netherlands

³ Quantib-U, Utrecht, The Netherlands

⁴ Image Sciences Institute, University Medical Center Utrecht and Utrecht University, Utrecht, The Netherlands

⁵ Department of Biomedical Engineering and Physics, Amsterdam University Medical Centers – location AMC, Amsterdam, The Netherlands

⁶ Department of Pediatric Endocrinology, Wilhelmina Children's Hospital, University Medical Center Utrecht, Utrecht, The Netherlands

[2]; and excess visceral fat deposition has been associated with a higher risk of metabolic syndrome and malignancy [3, 4]. Nevertheless, studies on pediatric body composition and its prognostic significance are limited.

Childhood sarcopenia is a novel concept that needs to be defined. Yet, low muscle mass and loss of muscle are highly prevalent in clinical settings (20–41% of children) [5–10] and are associated with increased morbidity [5, 8–14]. Importantly, the presence of sarcopenia is often overlooked when obtaining anthropometric measurements, particularly when excess body fat is present. In an era of increasing childhood obesity, sarcopenic obesity may be an underrecognized condition.

Currently, cross-sectional imaging (computed tomography [CT] and magnetic resonance imaging [MRI]) is considered the gold standard for body composition analysis. It provides direct anatomical measurements, allowing for the discrimination of separate skeletal muscle and fat (subcutaneous, visceral) distribution [15, 16]. Axial single-slice measurements of abdominal muscle and fat area have shown to reliably predict whole-body muscle and fat mass, respectively [17]. Automatic segmentation tools are increasingly utilized, which are less time-consuming than manual segmentation and less affected by intra- and interobserver variability [18–20].

From birth to adolescence, pediatric body composition changes rapidly due to physiological changes in longitudinal height, endocrine status and energy expenditure. Before these changing body composition measures can begin to have a meaningful prognostic impact, data on the normal variation in cross-sectional body composition are needed. There is a lack of data on values for total muscle and fat areas on cross-sectional imaging in European children.

This study aimed to evaluate an automatic tool for the segmentation of skeletal muscle and fat areas on pediatric CT scans and to provide data on the variation in body composition throughout childhood in a cohort of otherwise healthy Dutch children using automatic segmentation.

Materials and methods

Study population

All children, ages 1 to 17 years, who underwent an abdominal CT scan after high-energy trauma (high-impact falls and traffic accidents) at the emergency department of a single Dutch tertiary center, between August 2002 and April 2019, were identified as representative of the general pediatric population ($n=537$). No individual was scanned twice. Patients were excluded in case of evident anatomic anomalies or extensive post-traumatic changes that would prevent reliable segmentation. Clinical data of the patients were not available.

CT image acquisition

All patients received 2 ml/kg contrast medium Iopromide (Ultravist 300, Bayer Healthcare, Berlin, Germany) according to our trauma protocol. CT examinations were obtained with multidetector scanners: Mx8000 IDT 16, Brilliance 64, iQon Spectral or Brilliance iCT; (all Philips Medical Systems, Cleveland, OH). Exposure settings (range: 35–190 mAs and 80–120 kVp) were adjusted to patient size. Axial 4 mm slices were reconstructed and displayed with a standard abdominal soft tissue setting (window level: 30, window width: 400).

Automatic segmentation tool

The Quantib Body Composition tool was used for automatic segmentation [21, 22] (available online for scans of adults, <https://research.quantib.com>). As the method was developed for adult CTs, for this study, the networks of the slice selection and segmentation methods were retrained using a set of 49 manually-segmented images in children.

The segmentation method consisted of two steps. First, the automatic tool identified the slice at the craniocaudal midportion of the third lumbar vertebra (L3) from the CT data set using a convolutional neural network. Second, the automatic tool segmented the L3 slice into the following areas, using a second dilated convolutional neural network [23]: psoas, abdominal wall (rectus abdominis; transversus abdominis; internal and external obliques) and paraspinal (quadratus lumborum, erector spinae, multifidus, latissimus dorsi) muscles and subcutaneous and visceral fat. The third lumbar vertebra is the most commonly used level for body composition assessment in the literature [16, 24].

To minimize the influence of the exact slice that was selected, the automatic tool segmented a total of five slices around the detected L3 level, that is, two above and two below the center-L3 slice, and, therefore, averaged the area measurements over a range of 2 cm.

Manual segmentation

A total of 52 axial CT images (not used during training of the segmentation tool), selected from all age groups and sexes, were manually segmented by one trained observer (A.S., a final-year medical student with 3 months of experience in radiology) using Medical Imaging Interaction Toolkit (MITK) version 2018.04 (www.mitk.org) [25]. In case of uncertainty, a radiologist (P.A.d.J.) with 15 years of experience was consulted. To compute intra-observer agreement, 30 of the 52 scans were segmented twice by

the same observer, at least 12 months later, in a different order and blinded to previous results.

Evaluation of automatic segmentations

Manually-segmented CT images were used as the validation subset for automatic segmentation. Measurements of automatic and manual segmented areas were compared using the intraclass correlation coefficient (ICC) and Bland-Altman plots. To assess correct anatomical decision-making by the algorithm, Dice coefficients were computed between manual and automatic segmentations at the same slice, as well as between the intra-observer segmentations.

Normative data from automatic segmentations

To obtain normative data, CT scans of all 537 patients were processed with the automatic segmentation tool. Independent evaluation of all automatic segmentations was performed by another reviewer (S.S., with three years of experience in pediatric radiology research). The reviewer excluded all visually incorrect automatic segmentations, in terms of level and/or segmented areas and accepted only small segmentation errors, that would not result in important changes in area measurements. Descriptive statistics were used to report data in the form of median values and interquartile ranges (IQR). The analyses were stratified by sex and age. For each patient, the following ratios were calculated: visceral-to-subcutaneous fat, visceral-to-total fat and total muscle-to-fat area.

Correlations between continuous variables were calculated using Spearman's rho correlation coefficients. Student's *T*-tests were used to test the difference between means of continuous variables between the two sexes. Logarithmic transformations were applied to non-normally distributed variables. The data were analyzed using software (SPSS version 25, IBM, Armonk, NY and R Core Team 2017, R Foundation for Statistical Computing, Vienna, Austria). The *quantreg* package in R was used for the reconstruction of the quantile regression curves (R. Koenker [2020], <https://cran.r-project.org/package=quantreg>). *P*-values <0.05 were considered statistically significant.

Results

Automated and manual segmentation

For the 52 CT examinations used to validate the tool, the ICC between manually- and automatically-segmented areas was 0.98 (95% confidence interval [CI] 0.96–0.99) for total muscle area and 0.99 (95% CI 0.98–0.99) for total fat area ($P < 0.001$) (Fig. 1). Bland Altman plots

(Fig. 2) show that automatically-segmented measurements of visceral fat and total fat area are systematically higher than the manually-segmented measurements. Dice coefficients for manual vs. automatic segmentation were similar to the Dice coefficients of manual intra-observer variation (Table 1), with the highest variation for visceral fat.

Normative data

After automatic segmentation of the CT scans of all 537 patients, we excluded CT examinations of 44 patients for the following reasons: 17 because of abnormal anatomy (consisting of lumbosacral agenesis and muscular dystrophy) and/or extensive posttraumatic changes (consisting of burst fracture of L3, emphysema/hemorrhage of intraperitoneal space, visceral organs, muscles and/or subcutis) and 27 because of incorrect CT segmentations in terms of selected level or segmented areas. This resulted in a study sample of 493 children, ages 1 to 17 years, including 326 boys (66%) for the establishment of normative data. Age distribution was similar for both sexes, with a median age of 14 (IQR 9–17) years for boys and 14 (IQR 9–16) for girls.

Muscle and fat areas at the level of the third lumbar vertebra

Values (median and IQR, Tables 2 and 3) according to age and sex are summarized for L3 total muscle areas (Table 2) and visceral, subcutaneous and total fat area (Table 3). Corresponding quantile regression curves are plotted in Fig. 3 (curves for psoas, abdominal and long spine muscles in Supplementary Material 1, Fig. 1).

With increasing age, median total muscle area ranged from 38 cm² (IQR 31–39) to 174 cm² (IQR 160–190) in boys and from 41 cm² (IQR 38–43) to 127 cm² (IQR 123–138) in girls. A strong correlation between total muscle area and age was found for both sexes (Spearman's correlation coefficient 0.88 for boys and 0.85 for girls, both $P < 0.01$). Furthermore, psoas muscle area was strongly correlated with total muscle area for both sexes (0.94 for boys, 0.88 for girls, both $P < 0.01$).

With increasing age, median total fat area increased from 37 cm² (IQR 31–37) to 129 cm² (IQR 90–183) in boys and from 35 cm² (IQR 32–55) to 227 cm² (IQR 148–274) in girls. Total fat areas increased with age for both sexes (with a correlation coefficient of 0.61 for boys and 0.70 for girls, $P < 0.001$), especially during adolescence. A proportion (10%) of boys and girls begin to accumulate more fat tissue even before the average age for onset of puberty.

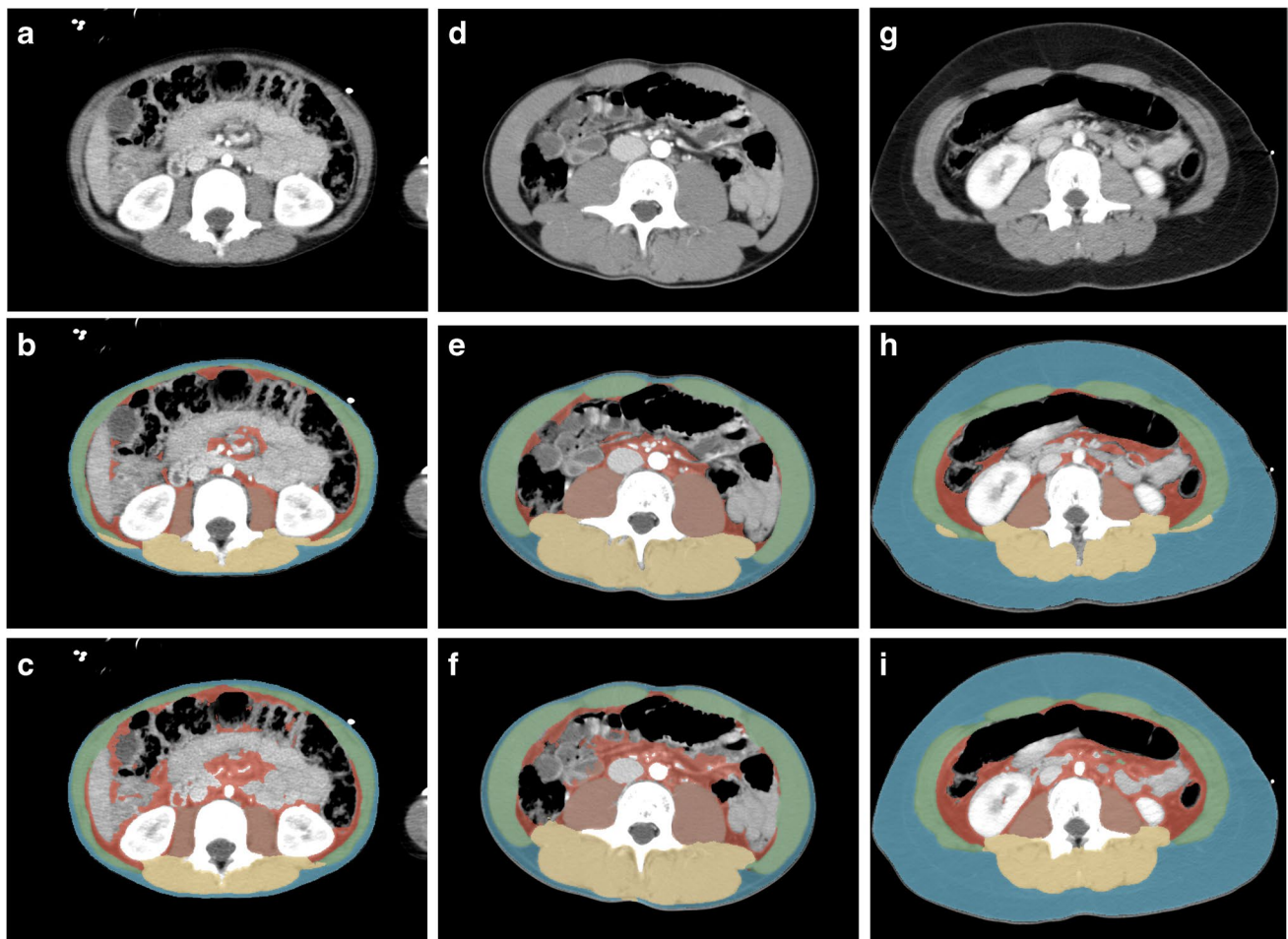


Fig. 1 Axial computed tomography images obtained in a 5-year-old boy (**a–c**), a 15-year-old boy (**d–f**) and a 12-year-old girl (**g–i**) at the level of the third lumbar vertebral body performed following high-energy trauma. Contrast-enhanced images before segmentation (**a, d, g**) and after manual (**b, e, h**) and automatic (**c, f, i**) seg-

mentation. Automatic segmentation sometimes included parts of the intestines as visceral fat and often failed to differentiate the abdominal wall muscles from the latissimus dorsi muscles. *Blue* subcutaneous fat, *green* abdominal wall muscles, *red* visceral fat, *orange* psoas muscles, *yellow* paraspinal muscles

Ratios

The ratio between visceral and subcutaneous fat decreased with age for both sexes and ranged between 0.1 and 3.5 for boys (median 1.1, IQR 0.7–1.5) and between 0.2 and 3.4 for girls (median 0.6, IQR 0.4–0.9). When comparing the ratio of visceral-to-subcutaneous fat between sexes, a mean difference of 0.4 ($P < 0.01$) in visceral-to-subcutaneous fat ratio was observed, indicating a higher percentage of visceral fat in boys than in girls throughout childhood. The total fat-to-muscle ratio ranged from 0.2 to 3.8 in boys (median 0.7, IQR 0.5–1.0) and from 0.4 to 3.9 in girls (median 1.0, IQR 0.8–1.7). The mean difference in total fat-to-muscle ratio between boys and girls was 0.4 ($P < 0.01$) with a higher mean ratio in girls. With increasing age, a subtle downward trend in total fat-to-muscle ratio was seen in boys, but a portion of boys exceeded values of 1.0 (Supplementary Material 2, Fig. 2).

Discussion

In this pilot study, an automatic segmentation tool for body composition was evaluated and used to provide data for total muscle and fat areas at the level of L3 in children undergoing CT after high-energy trauma. Mean Dice coefficients between manually- and automatically-segmented areas were high for muscle (0.87–0.90) and subcutaneous fat (0.88), but lower for visceral fat (0.60). As expected, around puberty boys start to gain more muscle mass compared to girls and the overall fat-to-muscle ratio is higher in girls compared to boys (median 1.01 vs. 0.65; $P < 0.01$). Approximately 10% of boys and girls begin to accumulate more fat tissue before the average age for onset of puberty. Our study demonstrates that even from a young age, boys appear more prone to visceral fat storage.

The performance of the automatic tool is generally good when compared with the intra-observer manual

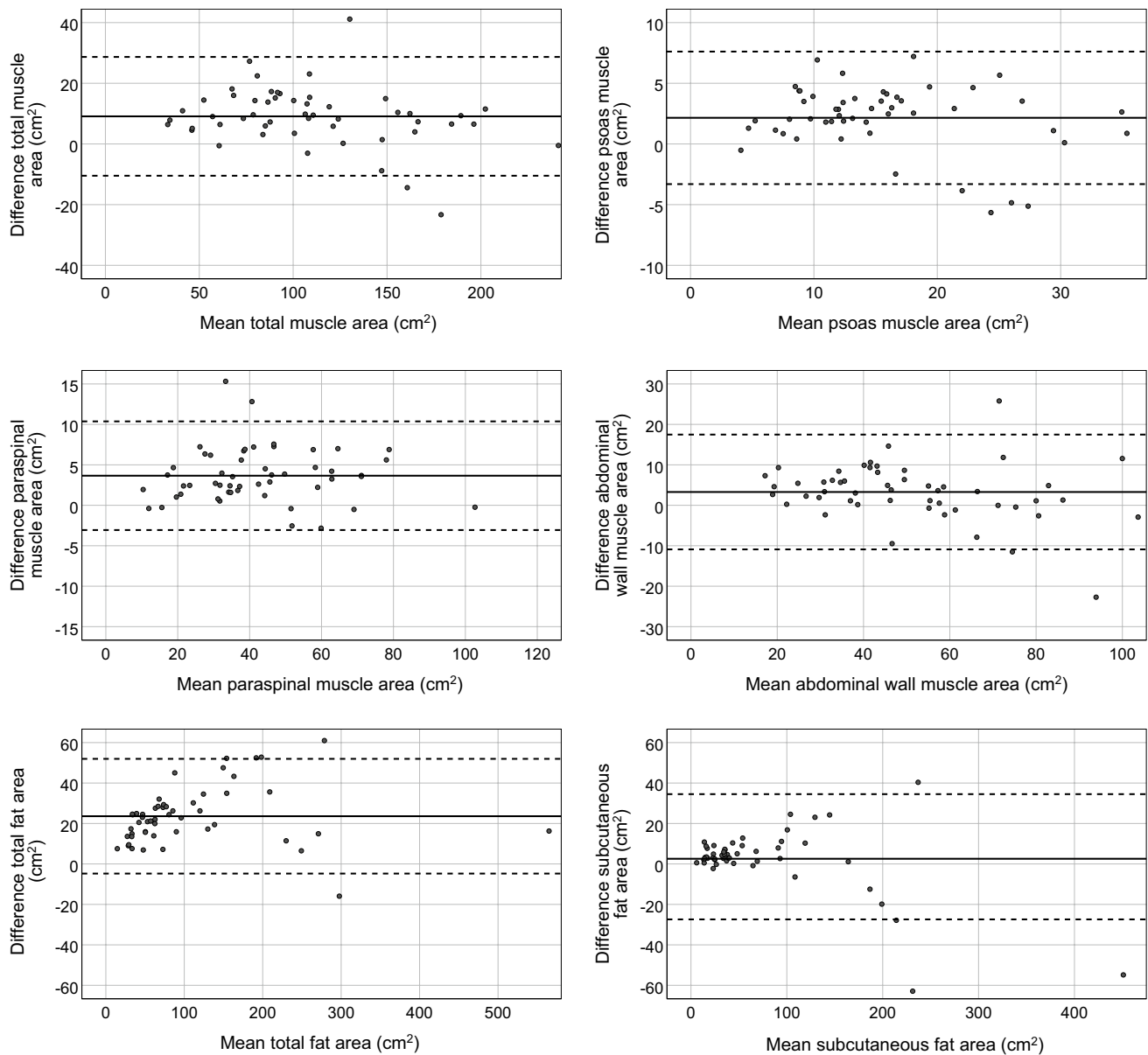


Fig. 2 Bland Altman plots comparing measurements by automatic and manual segmentation of muscle and fat areas in 52 children. The difference (automatic - manual) between the two measurements

(y-axis) is plotted against their average (x-axis). The broken lines represent the 95% confidence intervals of the average differences and the continuous line represents the mean difference

segmentations. The low intra-observer Dice coefficients for visceral fat (for both manual and automatic segmentation) demonstrate that visceral fat is the most difficult compartment to segment in children who have little visceral fat. The Bland-Altman analysis revealed systematically higher values of visceral fat area by automatic segmentation compared to manual segmentation. This may be for various reasons: (1) the automatic tool is more sensitive in segmenting small areas and therefore includes more small regions of visceral fat (see example in Fig. 1); (2) the automatic tool used the average of multi-slice segmentation vs. one-slice manual

segmentation. Multi-slice assessment may provide a more consistent representation of fat area, compared to one-slice measurement, especially for visceral fat area; (3) the automatic tool overestimates visceral fat at the cost of visceral organs (see example in Fig. 1). All in all, with 5% of the studies being excluded due to incorrect automatic segmentation, automatic segmentation should not be blindly applied without expert oversight and review.

Our L3 values were overall similar to age- and sex-specific measurements of psoas muscle areas at intervertebral spaces L3/L4 and L4/L5 [26] and L4 [27] in a cohort

Table 1 Dice coefficients for manual and automatic segmentation at the level of the third lumbar vertebral body

	Mean Dice coefficients ± standard deviation	
	Manual vs. manual segmentations (intra-observer)	Manual vs. automatic segmentation
Psoas muscles	0.90 ± 0.03	0.87 ± 0.06
Paraspinal muscles	0.91 ± 0.03	0.90 ± 0.04
Abdominal wall muscles	0.89 ± 0.03	0.87 ± 0.05
Subcutaneous fat	0.86 ± 0.10	0.88 ± 0.09
Visceral fat	0.67 ± 0.09	0.60 ± 0.09

representing children in North America (undergoing CT after trauma and/or appendicitis). Harbaugh et al. [27] also provided data for visceral fat area at L4 in children in the USA. Our IQR for visceral fat were higher than their data, which may be explained by the difference in level and over-estimation of visceral fat compared to manual segmentation in our cohort. Studies on multilevel measurements and comparisons between levels in children are limited. Further research comparing different levels in pediatric populations could be valuable for exploring potential variations and establishing standardized protocols.

We have provided insight into the timing of changes in body muscle and fat throughout childhood. While boys and girls have comparable fat and muscle area during early

Table 2 Muscle areas (psoas, paraspinal, abdominal wall and total) according to age and sex at the level of the third lumbar vertebra IQR inter-quartile range

Age, y	Boys (n=326)					Girls (n=167)				
	n (%)	Median (IQR) muscle area, cm ²				n (%)	Median (IQR) muscle area, cm ²			
		Psoas	Paraspinal	Abdominal wall	Total		Psoas	Paraspinal	Abdominal wall	Total
1	7 (2%)	5 (5–6)	11 (10–14)	19 (15–21)	38 (31–39)	1 (1%)	2	10	22	34
2	9 (3%)	7 (6–8)	17 (15–20)	20 (20–24)	43 (41–47)	7 (4%)	7	14	19	41
3	11 (3%)	7 (6–8)	20 (19–22)	24 (22–25)	51 (48–53)	5 (3%)	8	18	23	48
4	6 (2%)	8 (8–9)	23 (22–23)	26 (25–27)	57 (56–59)	4 (2%)	8	18	23	51
5	10 (3%)	9 (8–10)	23 (21–24)	31 (26–34)	64 (55–68)	5 (3%)	9	21	28	57
6	9 (3%)	12 (9–13)	32 (27–34)	36 (28–39)	78 (65–85)	7 (4%)	9	25	28	62
7	6 (2%)	12 (11–14)	33 (32–34)	35 (32–37)	81 (77–85)	8 (5%)	10	25	29	63
8	18 (6%)	12 (12–14)	33 (30–35)	36 (34–39)	81 (77–87)	10 (6%)	11	28	34	76
9	17 (5%)	14 (13–15)	36 (35–40)	45 (42–46)	93 (88–101)	3 (2%)	12	34	38	85
10	18 (6%)	14 (13–16)	38 (35–41)	42 (39–45)	95 (87–101)	6 (4%)	13	34	38	87
11	11 (3%)	16 (14–17)	40 (39–43)	44 (41–58)	101 (98–114)	12 (7%)	16	41	45	103
12	25 (8%)	17 (14–19)	45 (40–53)	53 (46–57)	115 (102–125)	6 (4%)	18	47	54	119
13	13 (4%)	21 (19–23)	50 (46–58)	55 (49–62)	122 (116–141)	15 (9%)	19	46	52	114
14	14 (4%)	25 (22–27)	64 (49–71)	69 (62–79)	158 (133–169)	15 (9%)	19	46	48	114
15	26 (8%)	26 (23–30)	67 (58–73)	71 (68–79)	165 (149–185)	20 (12%)	18	51	54	125
16	57 (18%)	28 (22–31)	69 (63–76)	72 (68–81)	172 (156–188)	14 (8%)	18	51	55	123
17	69 (21%)	29 (24–31)	72 (65–79)	74 (68–83)	174 (160–190)	29 (17%)	20	52	56	127

Table 3 Fat areas (subcutaneous, visceral and total) according to age and sex at the level of the third lumbar vertebra *IQR* interquartile range

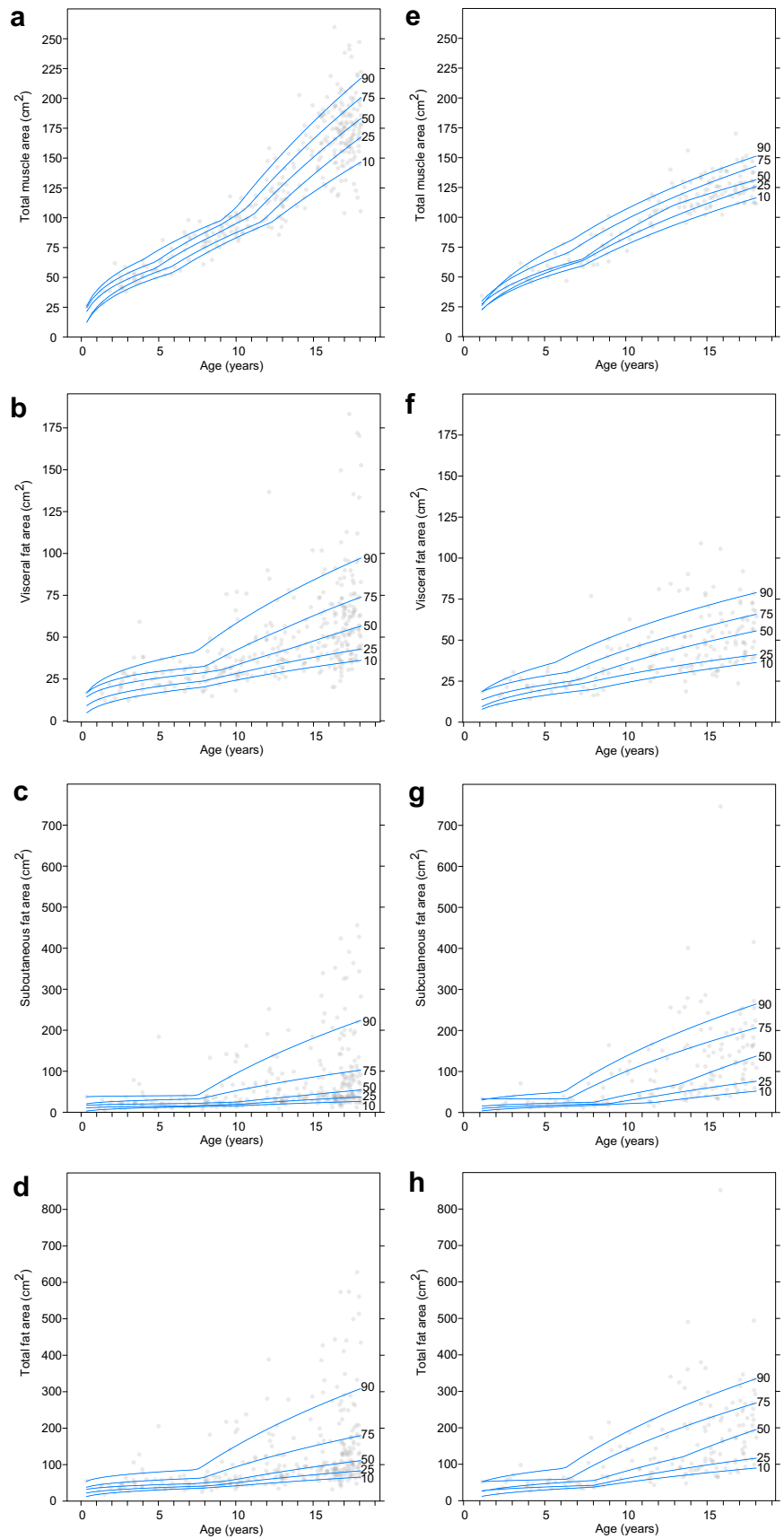
Age, y	Boys (n=326)				Girls (n=167)			
	n (%)	Median (IQR) fat areas, cm ²			n (%)	Median (IQR) fat areas, cm ²		
		Subcutaneous	Visceral	Total		Subcutaneous	Visceral	Total
1	7 (2%)	18 (15–28)	16 (13–18)	37 (31–37)	1 (1%)	34	19	53
2	9 (3%)	20 (10–22)	22 (20–27)	38 (34–46)	7 (4%)	19 (17–30)	17 (15–24)	35 (32–55)
3	11 (3%)	23 (19–37)	27 (20–33)	50 (39–72)	5 (3%)	29 (20–41)	23 (22–27)	51 (41–71)
4	6 (2%)	27 (16–30)	27 (25–29)	54 (38–59)	4 (2%)	16 (14–18)	19 (18–20)	35 (32–38)
5	10 (3%)	18 (15–21)	23 (21–29)	45 (36–56)	5 (3%)	21 (15–28)	25 (23–31)	51 (48–52)
6	9 (3%)	18 (15–32)	25 (21–30)	46 (39–58)	7 (4%)	28 (26–33)	24 (23–25)	56 (49–59)
7	6 (2%)	15 (14–17)	25 (19–29)	41 (37–44)	8 (7%)	21 (19–34)	24 (19–28)	44 (37–62)
8	18 (6%)	24 (23–34)	30 (25–33)	55 (49–67)	10 (6%)	25 (20–35)	31 (28–44)	66 (49–87)
9	17 (5%)	22 (17–65)	32 (29–39)	54 (48–100)	3 (2%)	94 (60–99)	44 (39–45)	139 (99–144)
10	18 (6%)	24 (19–52)	35 (28–38)	59 (47–95)	6 (4%)	86 (52–101)	47 (41–47)	124 (94–142)
11	11 (3%)	34 (22–65)	40 (36–49)	83 (59–118)	12 (7%)	51 (27–85)	34 (31–41)	83 (64–124)
12	25 (8%)	45 (27–94)	41 (33–53)	84 (66–150)	6 (4%)	98 (63–146)	49 (44–74)	146 (108–190)
13	13 (4%)	31 (27–58)	42 (36–52)	73 (63–101)	15 (9%)	66 (47–205)	41 (34–52)	112 (79–260)
14	14 (4%)	38 (34–57)	44 (36–56)	91 (71–95)	15 (9%)	68 (52–133)	46 (37–57)	107 (87–196)
15	26 (8%)	45 (36–100)	50 (41–65)	95 (82–164)	20 (12%)	95 (74–148)	45 (32–58)	139 (109–222)
16	57 (18%)	40 (32–93)	50 (37–67)	88 (72–157)	14 (8%)	95 (55–147)	49 (39–55)	142 (93–203)
17	69 (21%)	69 (38–110)	62 (47–76)	129 (90–183)	29 (17%)	165 (105–218)	58 (46–69)	227 (148–274)

childhood, a wider variance is observed during adolescence. We quantify that with the start of puberty, triggered by the gonadal hormones, boys generally gain more muscle and girls gain more fat. While the amount of visceral fat at birth is known to be negligible [28], we found that children start to accumulate visceral fat from a young age, even before the age of onset of puberty. This increase in fat accumulation may be partially explained by the physiological preparation for puberty. It is well-established that adult males have higher visceral-to-subcutaneous fat ratios and adult females have more subcutaneous fat and total fat [29]. In our cohort, these sex differences in fat distribution were present from a young age. This has also been described by several studies in children of various ages between four and eighteen years [30–33]. The timing of fat accumulation has important implications for future health, including the

risk of developing metabolic complications associated with excess adiposity [34].

Body composition analysis has broad relevance in primary and specialty healthcare settings. Normal values are important to identify children with abnormal body composition and to evaluate its prognostic impact. Altered body composition can affect the distribution and clearance of drugs [35, 36]. Children with aberrant body composition may be at risk for under- and overdosing. It should be studied whether personalized body composition-based dosing can minimize treatment toxicity and improve treatment efficacy [37]. In addition, whether improving body composition with supportive (nutritional and physical) interventions can improve outcomes, such as chemotherapy tolerance and quality of life, has yet to be studied in children.

Fig. 3 Quantile regression curves at the level of the third lumbar vertebra in boys (a–d) and girls (e–h) show total muscle (a, e) and visceral (b, f) subcutaneous (c, g) and total fat (d, h) areas according to age and sex. Observed 10th, 25th, 50th, 75th and 90th percentiles



The evaluation of an automatic segmentation tool provides a basis for further validation of body composition as a predictor of outcomes in many disease settings. It is important to establish reference and cut-off values for morphometric measures that can predict an increased risk of adverse outcomes. Cross-sectional imaging is often available in children in the clinical setting and holds important body compositional information. Cross-sectional imaging from, for example, trauma patients can serve as a representation of the general pediatric population. We should not scan children solely for the purpose of pediatric body composition analysis. We advocate for opportunistic use of these readily-available cross-sectional images for routine body composition assessment.

Some limitations of our study should be addressed. First, when interpreting the Dice coefficients, ICC and Bland Altman plots, it should be noted that only 52 scans were segmented manually and scans with visual abnormalities were not included. Second, for some age groups, the sample size per sex was not sufficient to determine reliable normative values, as older children (age 15–17 years) and boys (66%) were overrepresented in our study cohort. Third, some important parameters of body composition were not available, such as a history of chronic disease, pubertal stage or race/ethnicity. It would have been very informative to correlate CT measures to body mass index, but these data were not available because the height/weight of these children is not routinely measured in the trauma setting. Fourth, in this study, we included trauma patients from one single tertiary center in a relatively urban area as the best available representation of the general pediatric population. It could be that children that sustain high-energy trauma differ in body composition from the average child. The automatic tool was trained on a relatively small dataset from a single center, which may limit generalizability. Training the automatic tool using more manually-segmented scans from a more diverse dataset, including a wider range of factors such as age, anatomy, and scan acquisition parameters, could result in a more robust algorithm.

This pilot study demonstrates the pediatric application of an automatic tool for generating data for cross-sectional body composition. In a cohort of the Dutch pediatric population, we found important differences in both L3 muscle and fat areas according to sex and age. Knowledge of these values adds to our understanding of the physiologic changes in body composition that occur throughout childhood. It provides a basis for further studies on (early) identification of vulnerable children with aberrant body composition and evaluation of its possible health risks throughout life.

Conclusion

With the increasing use of cross-sectional imaging and the development of automated segmentation methods, it is only now that we can harvest the wealth of prognostic power that lies in body-compositional analyses. A logical next step is to not only analyze tissue volumes but include their make-up in terms of CT Hounsfield units, which will further increase the relevance and applicability of these measures.

Supplementary information Supplementary material is available at <https://doi.org/10.1007/s00247-023-05739-x>.

Author contributions A.S., S.S., P.A.d.J., R.A.J.N. and A.S.L. contributed to the study conception and design. A.S. and S.S. performed material preparation, data collection and analysis, as well as writing the first draft of the manuscript. All authors commented on previous versions of the manuscript. All authors read and approved the final manuscript.

Data availability Source data discussed in the article are available on e-mail request to the guarantors of this study.

Declarations

Ethics approval Ethical approval was waived by the local Ethics Committee of University Medical Center Utrecht (IRB official waiver number: 19-423) given the retrospective nature of the study and that all the procedures being performed were part of the routine care. Informed consent was waived due to the anonymous handling of retrospective data.

Conflicts of interest The automated segmentation tool was developed by Quantib-U. P. M. is an employee at Quantib-U; W.B.V. and B.D.d.V. are co-founders of Quantib-U. Employee authors had no influence on the study design, data interpretation or drafting of the manuscript and were not compensated aside from their salary. A.S., S.S., P.M., A.S.L., P.A.d.J., H.M.v.S. and R.A.J.N. declare that they have no relevant financial or non-financial interests to disclose.

Open Access This article is licensed under a Creative Commons Attribution 4.0 International License, which permits use, sharing, adaptation, distribution and reproduction in any medium or format, as long as you give appropriate credit to the original author(s) and the source, provide a link to the Creative Commons licence, and indicate if changes were made. The images or other third party material in this article are included in the article's Creative Commons licence, unless indicated otherwise in a credit line to the material. If material is not included in the article's Creative Commons licence and your intended use is not permitted by statutory regulation or exceeds the permitted use, you will need to obtain permission directly from the copyright holder. To view a copy of this licence, visit <http://creativecommons.org/licenses/by/4.0/>.

References

1. Lee MH, Zea R, Garrett JW et al (2022) Abdominal CT body composition thresholds using automated AI tools for predicting 10-year adverse outcomes. *Radiology* 306:e220574
2. Cruz-Jentoft AJ, Sayer AA (2019) Sarcopenia. *Lancet* 393:2636–2646. [https://doi.org/10.1016/S0140-6736\(19\)31138-9](https://doi.org/10.1016/S0140-6736(19)31138-9)
3. Fox CS, Massaro JM, Hoffmann U et al (2007) Abdominal visceral and subcutaneous adipose tissue compartments: association

- with metabolic risk factors in the Framingham Heart Study. *Circulation* 116:39–48
4. De Pergola G, Silvestris F (2013) Obesity as a major risk factor for cancer. *J Obes* 2013: <https://doi.org/10.1155/2013/291546>
 5. Ooi PH, Mazurak VC, Bhargava R, et al (2020) Myopenia and reduced subcutaneous adiposity in children with liver disease are associated with adverse outcomes. *J Parenter Enter Nutr* 0: <https://doi.org/10.1002/jpen.1963>
 6. Lurz E, Patel H, Frimpong RG et al (2018) Sarcopenia in children with end-stage liver disease. *J Pediatr Gastroenterol Nutr* 66:222–226
 7. Mangus RS, Bush WJ, Miller C, Kubal CA (2017) Severe sarcopenia and increased fat stores in pediatric patients with liver, kidney, or intestine failure. *J Pediatr Gastroenterol Nutr* 65:579–583
 8. Suzuki D, Kobayashi R, Sano H et al (2018) Sarcopenia after induction therapy in childhood acute lymphoblastic leukemia: its clinical significance. *Int J Hematol* 107:486–489
 9. Dedhia PH, White Y, Dillman JR et al (2018) Reduced paraspinous muscle area is associated with post-colectomy complications in children with ulcerative colitis. *J Pediatr Surg* 53:477–482
 10. Mager DR, Hager A, Ooi PH et al (2019) Persistence of sarcopenia after pediatric liver transplantation is associated with poorer growth and recurrent hospital admissions. *J Parenter Enter Nutr* 43:271–280
 11. Kawakubo N, Kinoshita Y, Souzaki R et al (2019) The influence of sarcopenia on high-risk neuroblastoma. *J Surg Res* 236:101–105
 12. Rayar M, Webber CE, Nayiager T et al (2013) Sarcopenia in children with acute lymphoblastic leukemia. *J Pediatr Hematol Oncol* 35:98–102
 13. Marriott CJ, Beaumont LF, Farncombe TH et al (2018) Body composition in long-term survivors of acute lymphoblastic leukemia diagnosed in childhood and adolescence: a focus on sarcopenic obesity. *Cancer* 124:1225–1231
 14. Takeda M, Sakamoto S, Uchida H et al (2020) Impact of sarcopenia in infants with liver transplantation for biliary atresia. *Pediatr Transplant* 1–9. <https://doi.org/10.1111/ptr.13950>
 15. Cruz-Jentoft AJ, Bahat G, Bauer J et al (2019) Sarcopenia: revised European consensus on definition and diagnosis. *Age Ageing* 48:16–31
 16. Thomas EL, Fitzpatrick JA, Malik SJ et al (2013) Whole body fat: content and distribution. *Prog Nucl Magn Reson Spectrosc* 73:56–80
 17. Shen W, Punyanitya M, Wang ZM et al (2004) Total body skeletal muscle and adipose tissue volumes: Estimation from a single abdominal cross-sectional image. *J Appl Physiol* 97:2333–2338
 18. Weston AD, Korfiatis P, Kline TL et al (2019) Automated abdominal segmentation of CT scans for body composition analysis using deep learning. *Radiology* 290:669–679
 19. Magudia K, Bridge CP, Bay CP, et al (2020) Population-scale CT-based body composition analysis of a large outpatient population using deep learning to derive age-, sex-, and race-specific reference curves. *Radiology* 201640. <https://doi.org/10.1148/radiol.2020201640>
 20. Graffy PM, Liu J, Pickhardt PJ, et al (2019) Deep learning-based muscle segmentation and quantification at abdominal CT: application to a longitudinal adult screening cohort for sarcopenia assessment. *Br J Radiol* 92: <https://doi.org/10.1259/bjr.20190327>
 21. Moeskops P, de Vos BD, Veldhuis WB et al (2020) Automatic quantification of body composition at L3 vertebra level with convolutional neural networks. *Eur. Congr. Radiol*, In
 22. Van Erck D, Moeskops P, Schoufour JD et al (2022) Evaluation of a fully automatic deep learning-based method for the measurement of psoas muscle area. *Front Nutr* 9:1–8
 23. Yu F, Koltun V (2016) Multi-scale context aggregation by dilated convolutions. In: 4th International Conference on Learning Representations, ICLR 2016 - Conference Track Proceedings
 24. Castiglione J, Somasundaram E, Gilligan LA et al (2021) Automated segmentation of abdominal skeletal muscle on pediatric CT scans using deep learning. *Radiol Artif Intell* 3:e200130
 25. Wolf I, Vetter M, Wegner I et al (2005) The medical imaging interaction toolkit. *Med Image Anal* 9:594–604
 26. Lurz E, Patel H, Lebovic G et al (2020) Paediatric reference values for total psoas muscle area. *J Cachexia Sarcopenia Muscle* 11:405–414
 27. Harbaugh CM, Zhang P, Henderson B et al (2017) Personalized medicine: enhancing our understanding of pediatric growth with analytic morphomics. *J Pediatr Surg* 52:837–842
 28. Harrington TAM, Thomas EL, Frost G et al (2004) Distribution of adipose tissue in the newborn. *Pediatr Res* 55:437–441
 29. Schorr M, Dichtel LE, Gerweck AV et al (2018) Sex differences in body composition and association with cardiometabolic risk. *Biol Sex Differ* 9:1–10
 30. Staiano AE, Broyles ST, Gupta AK, Katzmarzyk PT (2013) Ethnic and sex differences in visceral, subcutaneous, and total body fat in children and adolescents. *Obesity* 21:1251–1255
 31. Shen W, Punyanitya M, Silva AM et al (2009) Sexual dimorphism of adipose tissue distribution across the lifespan: a cross-sectional whole-body magnetic resonance imaging study. *Nutr Metab* 6:1–9
 32. Lee S, Kuk JL, Hannon TS, Arslanian SA (2008) Race and gender differences in the relationships between anthropometrics and abdominal fat in youth. *Obesity* 16:1066–1071
 33. Benfield LL, Fox KR, Peters DM et al (2008) Magnetic resonance imaging of abdominal adiposity in a large cohort of British children. *Int J Obes* 32:91–99
 34. Gallagher D, Andres A, Fields DA et al (2020) Body composition measurements from birth through 5 years: challenges, gaps, and existing & emerging technologies—a National Institutes of Health workshop. *Obes Rev* 21:1–15
 35. Bauer J, Jürgens H, Frühwald MC (2011) Important aspects of nutrition in children with cancer. *Adv Nutr* 2:67–77
 36. Antoun S, Borget I, Lanoy E (2013) Impact of sarcopenia on the prognosis and treatment toxicities in patients diagnosed with cancer. *Curr Opin Support Palliat Care* 7:383–389
 37. de Jong DJ, Veldhuis WB, Wessels FJ et al (2021) Towards personalised contrast injection: artificial-intelligence-derived body composition and liver enhancement in computed tomography. *J. Pers. Med*, p 11

Publisher's note Springer Nature remains neutral with regard to jurisdictional claims in published maps and institutional affiliations.